Surface tension of electrolytes: Hydrophilic and hydrophobic ions near an interface

Akira Onuki[a)]
Department of Physics, Kyoto University, Kyoto 606-8502, Japan

(Received 19 March 2008; accepted 6 May 2008; published online 12 June 2008)

We calculate the ion distributions around an interface in fluid mixtures of highly polar and less polar fluids (water and oil) for two and three ion species. We take into account the solvation and image interactions between ions and solvent. We show that hydrophilic and hydrophobic ions tend to undergo a microphase separation at an interface, giving rise to an enlarged electric double layer. We also derive a general expression for the surface tension of electrolyte systems, which contains a negative electrostatic contribution proportional to the square root of the bulk salt density. The amplitude of this square-root term is small for hydrophilic ion pairs but is much increased for hydrophilic and hydrophobic ion pairs. For three ion species, including hydrophilic and hydrophobic ions, we calculate the ion distributions to explain those obtained by x-ray reflectivity measurements. © *2008 American Institute of Physics*. [DOI: 10.1063/1.2936992]

I. INTRODUCTION

It has long been known that the surface tension γ of a water-air interface increases with addition of inorganic salts in water. Wagner[1] ascribed its origin to the image charge in air due to the difference in the dielectric constants of the two phases, which repels each ion in water away from the interface. Onsager and Samaras[2] obtained the limiting law for the surface tension change in the form $\Delta\gamma=\frac{1}{8}Tn_w\ell_B[\ln(1/n_w\ell_B^3)+\text{const}]$, where $n_w(\ll\ell_B^{-3})$ is the ion density in the bulk water and ℓ_B is the Bjerrum length. Levin and Flores-Mena[3] took account of ion depletion due to a relatively large size of the hydration shell radius.[4] In experiments, at not extreme dilution, the linear behavior $\Delta\gamma=Tn_w\lambda_s$ has been measured,[5–8] where λ_s is the effective thickness of the ion-free layer. For example, for NaCl, $\lambda_s\sim 3$ Å, where the densities of Na^+ and Cl^- are $n_w/2$. However, for a number of salts around 1 mM in aqueous solutions, Jones and Ray[5] detected a very small negative minimum in $\Delta\gamma$, which still remains an unsolved controversy.[8–10]

In polar fluid mixtures, the ion distributions are much more complicated when the ions are soluble in the two phases.[11–13] In this problem, we need to account for the solvation between ions and solvent molecules (hydration in aqueous solutions), whose free energy contribution usually much exceeds the thermal energy T (per ion).[4] In particular, one ion species can prefer one fluid component, while the other species can prefer the other component. Such asymmetric ion pairs tend to segregate around an interface, while the segregation is prohibited on larger scales due to the charge neutrality in the bulk. In this paper, we will examine this microphase separation near an interface to calculate a decrease in the surface tension $\Delta\gamma<0$, whose amplitude can be much larger than that of the well-known increase for hydrophilic ion pairs. It is worth noting that, in their small-angle neutron scattering experiment, Sadakane *et al.*[14] found periodic charge-density-wave structures in a near-critical binary mixture of D_2O-trimethylpyridine containing sodium tetraphenylborate ($NaBPh_4$). Their salt is composed of a strongly hydrophilic cation Na^+ and a strongly hydrophobic anion BPh_4^-, which should considerably decrease the surface tension and produce a mesoscopic structure near the critical point.

In their x-ray reflectivity experiment, Luo *et al.*[15] measured the ion distributions in the vicinity of an interface in water-nitrobenzene. They added two salts, tetrabutylammonium tetraphenylborate (TBA-TPB) and tetrabutylammonium bromide (TBA-Br). Then, they realized a two-phase state with hydrophilic anion Br^-, hydrophobic cation TBA^+, and hydrophobic anion TPB^-. They detected a strong accumulation or depletion of the ions on the two sides of the interface, which suggests the crucial role of the ion-solvent interactions dependent on the ion and solvent species. In water-nitrobenzene containing both hydrophilic and hydrophobic ions, a large drop of the surface tension has been observed.[11,15]

We mention the presence of a large body of spectroscopic experiments and computer simulations with molecular resolution on ion effects at a water-air interface,[16,17] where the air region may be treated as a vacuum. Such studies provide detailed information of ionic interfacial behavior on the angstrom scale for various ion species. However, microscopic studies remain inadequate for ion effects at a water-oil interface. On the contrary, in this paper, our approach will be based on a Ginzburg–Landau theory of solvation and ion distributions.[12,13] We will consider water-oil systems such as water-nitrobenzene, where the dielectric constants of the two components are not much separated (the dielectric constant of nitrobenzene is about 35).

This paper is organized as follows. In Sec. II, we will present a Ginzburg–Landau approach to the molecular interactions between ions and solvent molecules. Taking account

a)Electronic mail: onuki@scphys.kyoto-u.ac.jp.

of the electrostatic, solvation, and image interactions, we will introduce the grand potential and present a theoretical expression for the surface tension. It contains a negative electrostatic correction, which is not included in the Gibbs theory[18,19] but is crucial for hydrophilic and hydrophobic ion pairs. In Sec. III, we will numerically examine the ion distributions and the surface tension for hydrophilic and hydrophobic ion pairs. We will also discuss the behavior of $\Delta\gamma$ in the usual case of hydrophilic ion pairs in extreme dilution. In Sec. IV, we extend our theory in the presence of three ion species to explain the experiment by Luo *et al.*[15] In Appendix A, we will examine the relationship of our surface tension formula and the Gibbs equation. In Appendix B, we will relate our grand potential to the bulk pressure and derive the Laplace law using our surface tension formula since we will treat incompressible binary mixtures in the text.

II. THEORETICAL BACKGROUND

A. Ginzburg–Landau free energy

We consider a polar binary mixture containing a small amount of salt. The volume fraction of the more polar component is written as ϕ. The other less polar component has the volume fraction $1-\phi$. We neglect the volume fractions of the ions. The ion densities are written as $n_1, n_2, \ldots$. Their charges are $Z_i e$, so $Z_1=1$ and $Z_2=-1$ for two monovalent ion species. In our scheme, ϕ, $n_1, n_2, \ldots$, are smooth space-dependent variables coarse-grained on the microscopic level. We examine the ion distribution around an interface,[13] where all the quantities change along the z axis. The solvent molecular sizes are given by a common length a for the two components. Then, ϕ also represents the molar concentration. The interface thickness ξ is assumed to be longer than a. We neglect the formation of dipole pairs and ion clusters, which is relevant at not small ion densities.[20–22]

The free energy F of our system is the space integral of the free energy density f of the form

$$f = f_0(\phi,T) + \frac{C}{2}|\nabla\phi|^2 + \frac{\varepsilon(\phi)}{8\pi}E^2 + T\sum_i n_i[\ln(n_i a^3) - g_i\phi] + \mu_{\rm im}\sum_i Z_i^2 n_i. \tag{2.1}$$

We set the Boltzmann constant equal to unity. The first term f_0 is the chemical part in the Bragg–Williams form

$$f_0 = \frac{T}{a^3}[\phi\ln\phi + (1-\phi)\ln(1-\phi) + \chi\phi(1-\phi)], \tag{2.2}$$

where χ depends on the temperature T and its critical value is 2 in the absence of ions.[23,24] The second term is the gradient part, while the third term is the electrostatic free energy with Φ being the electric potential. The electrostatic potential Φ satisfies $\nabla\cdot\varepsilon(\phi)\nabla\Phi=-4\pi\rho$, where $\rho=\Sigma_i Z_i e n_i$ is the charge density. Around an interface, the electric field $E=-d\Phi/dz$ is expressed as

$$E(z) = \frac{4\pi}{\varepsilon(\phi(z))}\int_{-\infty}^{z} dz'\rho(z'), \tag{2.3}$$

where the lower bound of the integration is pushed to $-\infty$. The dielectric constant ε is assumed to be of the linear form[25]

$$\varepsilon(\phi) = \varepsilon_c + \varepsilon_1(\phi-\phi_c), \tag{2.4}$$

where ε_c and ε_1 are constants. ϕ_c is the critical volume fraction [$=1/2$ for the free energy density in Eq. (2.2)]. Thus, $\varepsilon(\phi)$ depends on z near an interface. The coupling terms $-Tg_i n_i\phi$ arise from the composition dependence of the solvation chemical potentials.[13] The differences $Tg_i\Delta\phi$ may be equated to the Gibbs transfer energies (per particle here) known in electrochemistry,[11,26–29] where $\Delta\phi$ is the concentration difference between the two phases. From the data of room-temperature water-nitrobenzene in strong segregation,[30] g_i are expected to be typically of the order of 15 for monovalent hydrophilic ions and are even larger for multivalent ions such as Ca^{2+} or Al^{3+}. For the hydrophobic anion BPh_4^- (tetraphenylborate), for example, it is about -15, on the other hand. The resultant solvation coupling between the ions and the composition is thus very strong, dramatically affecting the phase transition behavior near the critical point.[12,13] In binary mixtures, in which the more polar component is water, the coupling constants g_i are positive for hydrophilic ions and negative for hydrophobic ions.

The last term in Eq. (2.1) represents the image interaction, arising from inhomogeneous dielectric constant ε. It originates from the discrete nature of ions, while the electric field Φ in our theory is produced by the smoothly coarse-grained charge density ρ. The original papers[1,2] treated water-air interfaces, but we suppose weak or moderate inhomogeneity of the dielectric constant across a diffuse interface. Then, it follows the Cauchy integral form[13]

$$\mu_{\rm im}(z) = TAa\frac{\varepsilon_1}{\varepsilon_c}\int\frac{dz'}{\pi}\frac{e^{-2\kappa|z-z'|}}{z-z'}\frac{d\phi(z')}{dz'}, \tag{2.5}$$

to first order in ε_1. The coefficient A represents the charge strength as

$$A = \pi e^2/4a\varepsilon_c T = \pi\ell_{Bc}/4a \tag{2.6}$$

where $\ell_{Bc}=e^2/\varepsilon_c T$ is the Bjerrum length at $\varepsilon=\varepsilon_c$. The damping factor $e^{-2\kappa|z-z'|}$ in Eq. (2.5) arises from the screening of the potential by the other ions.[1,2] In our numerical analysis, we treat κ as the space-dependent local value $[4\pi e^2 m(\boldsymbol{r})/\varepsilon(\boldsymbol{r})T]^{1/2}$ with $m=\Sigma_i Z_i^2 n_i$.

At equilibrium, we assume homogeneity of the chemical potentials $\mu_i=\delta F/\delta n_i$ $(i=1,2,\ldots)$ and $h=\delta F/\delta\phi$. We introduce normalized ion densities,[31]

$$c_i = a^3 n_i \quad (i=1,2,\ldots). \tag{2.7}$$

In our theory, the ion volume fractions are assumed to be so small such that the real ion sizes do not come into play. Since we have

$$\mu_i = T(\ln c_i + 1 - g_i\phi) + Z_i^2\mu_{\rm im} + Z_i e\Phi, \tag{2.8}$$

the ion density profiles are expressed as

$$\frac{c_i(z)}{c_{i0}} = \exp\left[g_i\phi(z) - \frac{Z_i e}{T}\Phi(z) - \frac{Z_i^2}{T}\mu_{\rm im}(z) \right], \tag{2.9}$$

where $c_{i0}=\exp(\mu_i/T-1)$. Taking the derivatives of the image free energy $F_{im}=\int d\boldsymbol{r}\mu_{\rm im}\Sigma_i Z_i^2 n_i$ with respect to n_i, we neglect the n-dependence of $\mu_{\rm im}$ in Eq. (2.5). $h=\delta F/\delta\phi$ has the meaning of the chemical potential difference of the two fluid components (divided by a^3). It is of the form

$$h = f_0'(\phi) - C\phi'' - \frac{\varepsilon_1}{8\pi}E^2 - T\sum_i g_i n_i + h_{\rm im}, \tag{2.10}$$

where $f_0'=\partial f_0/\partial\phi$ and $\phi''=d^2\phi/dz^2$. From the image interaction, we have the contribution $h_{\rm im}=\delta F_{\rm im}/\delta\phi$. In the one-dimensional (1D) case, $h_{\rm im}$ is given by the right-hand side of Eq. (2.5) with $d\psi(z')/dz'$ being replaced by $\Sigma_i Z_i^2 dn_i(z')/dz'$.

Hereafter, the quantities with the subscript α (the subscript β) denote the bulk values in the more (less) polar phase attained as $z\to-\infty$ (as $z\to\infty$). We assume that the screening lengths, κ_α^{-1} and κ_β^{-1}, are much shorter than the system length L. In real systems, this might not be the case for extremely small n_β. From Eq. (2.9), the distribution ratio of each ion can be expressed as

$$c_{i\beta}/c_{i\alpha} = \exp[Z_i e\Delta\Phi/T - g_i\Delta\phi], \tag{2.11}$$

where $\Delta\phi=\phi_\alpha-\phi_\beta$. The image interaction vanishes far from the interface and does not appear in Eq. (2.11). There arises a Galvani potential difference $\Delta\Phi=\Phi_\alpha-\Phi_\beta$ across an interface. This is determined by the charge neutrality far from the interface,

$$\sum_i Z_i c_{i\alpha} = \sum_i Z_i c_{i\beta} = 0. \tag{2.12}$$

In addition, as $z\to\pm\infty$, the homogeneity of h in Eq. (2.10) yields the bulk relations,

$$h = f_0'(\phi_\alpha) - T\sum_i g_i n_{i\alpha} = f_0'(\phi_\beta) - T\sum_i g_i n_{i\beta}. \tag{2.13}$$

B. Image interaction

We give more discussions on the image interaction. From Eq. (2.9), image interaction is important under the condition,[13]

$$\xi < Z_i^2 \ell_{Bc}\varepsilon_1\Delta\phi/4\varepsilon_c < \kappa^{-1}, \tag{2.14}$$

where $\kappa=\kappa_\alpha$ or κ_β in the two phases. When ions are present only in the more polar phase under Eq. (2.14), the change in the surface tension obeys the Onsager–Samaras law.[2] In the thin interface limit $\xi\to0$, Levin and Flores-Mena[3] argued that ions in water cannot approach the interface within the distance of the hydration shell radius $R_{\rm shell}^i$(Ref. 4) (on the order of the size of a water molecule). In our scheme, for finite interface thickness ξ, hydrophilic ions are repelled from an interface into the α region due to the solvation interaction [due to the factor $e^{g_i\phi}$ in Eq. (2.9) for $g_i>0$]. Thus, even in the absence of the image interaction, a depletion layer of hydrophilic ions can be formed and the linear behavior $\Delta\gamma\propto n_\alpha$ still follows. To make qualitative arguments, therefore, the image interaction may be neglected for not very large A in Eq. (2.6).

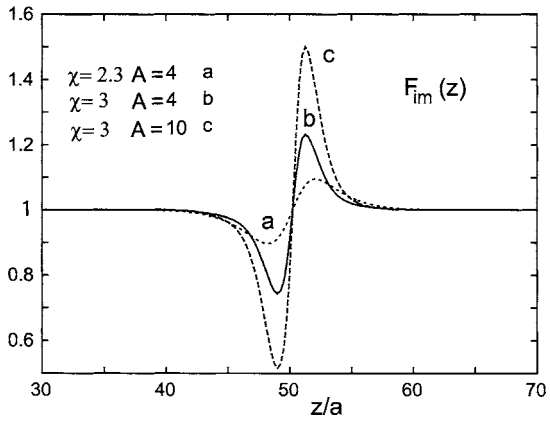

FIG. 1. The image factor $F_{\rm im}(z)$ for monovalent ions around an interface for (a) $\chi=2.3$ and $A=4$, (b) $\chi=3$ and $A=4$, and (c) $\chi=3$ and $A=10$, where $c_{1\alpha}=c_{1\beta}=2\times10^{-4}$.

In Fig. 1, we show examples of the image factor for monovalent ions near an interface,

$$F_{\rm im}(z) = \exp[-\mu_{\rm im}(z)/T], \tag{2.15}$$

which is calculated from Eq. (2.5) for $\varepsilon_1/\varepsilon_c=0.8$ and $\chi=3$. This factor appears in Eq. (2.9) for $Z_i=\pm1$. It is smaller than unity in the α region and is larger than unity in the β region since the image potential is repulsive in the α region and is attractive in the β region (see Appendix B of our previous paper[13]). At low densities, its minimum and maximum are more enhanced for larger $A\sim\ell_{Bc}/a$ and for larger χ (larger $\Delta\phi$), in accord with Eq. (2.14). See also analysis of the image interaction in our previous work.[13]

C. Surface tension

In order to calculate the surface tension, we introduce the grand potential density,

$$\omega = f - \sum_i \mu_i n_i - h\phi, \tag{2.16}$$

where f is given by Eq. (2.1). The space integral of ω is minimized under the given boundary conditions in equilibrium. In Appendix B, we will examine how $\omega(z)$ is related to the bulk pressure and the surface tension. We shall see that the discontinuity of ω across the interface $\omega_\alpha-\omega_\beta$ is nearly equal to the minus of the pressure discontinuity $p_\beta-p_\alpha$ in equilibrium. For a planar interface, we have $\omega_\alpha=\omega_\beta=\omega_\infty$.

Using Eq. (2.1) and eliminating μ_i with the aid of Eq. (2.8), we obtain

$$\omega = f_0 + \frac{C}{2}|\nabla\phi|^2 - h\phi - Tn + \frac{\varepsilon(\phi)}{8\pi}E^2 - \rho\Phi, \tag{2.17}$$

where $n=\Sigma_i n_i$ is the total ion density. Since $\omega(z)\to\omega_\infty$ as $z\to\pm\infty$ for a planar interface, h is expressed as

$$h = [f_0(\phi_\alpha) - f_0(\phi_\beta)]/\Delta\phi - T\Delta n/\Delta\phi, \tag{2.18}$$

where $\Delta n=n_\alpha-n_\beta$. With Eqs. (2.13) and (2.18), the bulk volume fractions ϕ_α and ϕ_β are determined for the given bulk ion densities (see Appendix A). The surface tension is ex-

pressed as $\gamma=\int dz[\omega(z)-\omega_\infty]$ (see Appendix B). It consists of two contributions as $\gamma=\gamma_1+\gamma_e$, with

$$\gamma_1=\int dz\left[f_0(\phi)+\frac{C}{2}\phi'^2-h\phi-Tn-C_\alpha\right], \tag{2.19}$$

$$\gamma_e=-\frac{1}{2}\int dz\rho\Phi=-\frac{1}{8\pi}\int dz\varepsilon(\phi)E^2, \tag{2.20}$$

where $\phi'=d\phi/dz$ and $C_\alpha=f_0(\phi_\alpha)-h\phi_\alpha-Tn_\alpha$. From Eq. (2.18), the integrand of Eq. (2.19) vanishes in the bulk α and β regions. The lower and upper bounds of the integrations in Eqs. (2.19) and (2.20) are pushed to infinity.

Here, it is convenient to introduce the excess adsorption Γ of the ions onto the interface by

$$\Gamma=\int dz\left[n-n_\alpha-\frac{\Delta n}{\Delta\phi}(\phi-\phi_\alpha)\right]$$
$$=\int_0^{z_{\rm int}}dz(n-n_\alpha)+\int_{z_{\rm int}}^{L}dz(n-n_\beta). \tag{2.21}$$

In the first line, the integrand vanishes far from the interface. In the second line, we suppose a finite system in the region $0<z<L$ with $L\gg\xi$ and determine the interface position by $z_{\rm int}=\int_0^L dz[\phi(z)-\phi_\beta]/\Delta\phi$. In Appendix A, we shall see that γ_1 is related to Γ at low ion densities by

$$\Delta\gamma_1=\gamma_1-\gamma_0\cong-T\Gamma, \tag{2.22}$$

where γ_0 is the surface tension without ions. The so-called Gibbs adsorption equation[19] relates the surface tension and the excess adsorption by $(\partial\gamma/\partial\ln n)_T=-T\Gamma$, where n is the number density of the doped particles (the ion density in our case). This equation yields Eq. (2.22) if $\Gamma\propto n$ and if γ_e is neglected. In our problem, however, Eq. (2.22) can be derived even if Γ is not a linear function of n (as in Fig. 3).

The γ_e in Eq. (2.20) is the minus of the z integration of the electrostatic energy density $f_{\rm el}=\varepsilon E^2/8\pi$. It arises from the last two terms in Eq. (2.17) with the aid of $\int dz\rho\Phi=\int dz\varepsilon(\phi)E^2/4\pi$. In all the examples in our previous work,[13] it was at most a few percents of $\Delta\gamma=\gamma-\gamma_0$. However, in the low density limit, we shall see that γ_e is proportional to the square root of the ion density. Moreover, its magnitude will turn out to be enlarged for strongly hydrophilic and hydrophobic ion pairs. This square-root dependence can be understood easily as follows. For simplicity, if $|g_1|$ and $|g_2|$ are of the order of unity, the screening lengths in the two phases are of the same order and $\Phi(z)$ changes from Φ_α to Φ_β smoothly on the scale of the screening length $\kappa_\alpha^{-1}\sim\kappa_\beta^{-1}$. Thus, $E(z)\sim\Delta\Phi\kappa_\alpha$ for $|z|\lesssim 1/\kappa_\alpha$ and $\gamma_e\sim-(\Delta\Phi)^2\varepsilon_\alpha\kappa_\alpha/4\pi$.

III. TWO SPECIES OF IONS

In the presence of two species of ions, where $Z_1>0$ and $Z_2<0$, we have the common density ratio $n_{1\alpha}/n_{1\beta}=n_{2\alpha}/n_{2\beta}$. In terms of $g_i\Delta\phi$, the ion density ratios and the Galvani potential difference are given by

$$\frac{n_{1\alpha}}{n_{1\beta}}=\exp\left[\frac{|Z_2|g_1+Z_1g_2}{Z_1+|Z_2|}\Delta\phi\right], \tag{3.1}$$

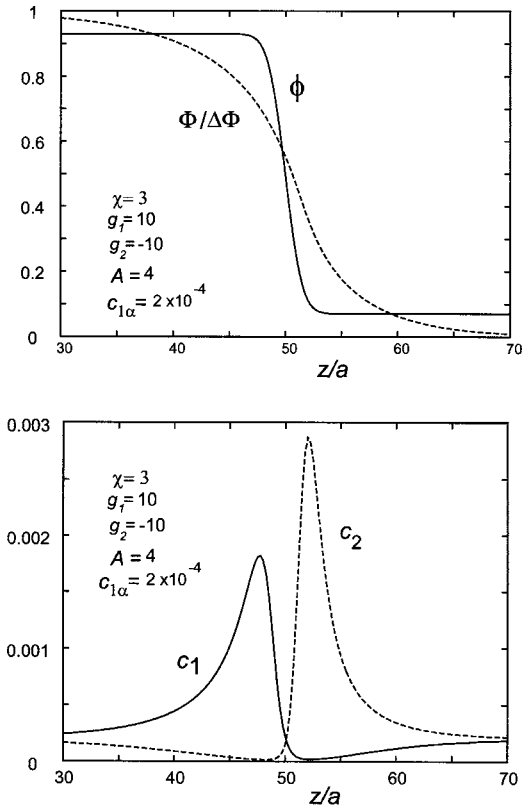

FIG. 2. The normalized electric potential $\Phi(z)/\Delta\Phi$ and composition $\phi(z)$ (upper panel), and normalized ion densities $c_1(z)$ and $c_2(z)$ (lower panel), where $\chi=3$, $A=4$, $g_1=-g_2=10$, and $c_{1\alpha}=c_{1\beta}=2\times10^{-4}$. For this pair of hydrophilic and hydrophobic ions, a microphase separation forming a large electric double layer is apparent.

$$\frac{e}{T}\Delta\Phi=\frac{g_1-g_2}{Z_1+|Z_2|}\Delta\phi. \tag{3.2}$$

The Galvani potential difference is created by an electric double layer at the interface. There is no electric field for the symmetric case $g_1=g_2$ in our theory. The potential $\Phi(z)$ changes on the scale of κ_α^{-1} in the α region and on the scale of κ_β^{-1} in the β region far from the interface at low ion densities. When $\kappa_\beta^{-1}\to\infty$ (as in the water-air case), $\Phi(z)-\Phi_\alpha$ becomes very small around the interface, changing slowly in the β region,[13] as has been assumed in literature.[1–3]

A. Numerical results

We numerically seek equilibrium interface solutions of Eqs. (2.8) and (2.10) for $C=\chi$ and $\varepsilon_1/\varepsilon_c=0.8$, as in our previous work.[13] Hereafter, $c_{1\alpha}=c_{2\alpha}$ and $c_{1\beta}=c_{2\beta}$ in the monovalent case. We set $\chi=3$ and $A=4$, except in Figs. 1 and 8. We have $\gamma_0=0.497T/a^2$ without salt and $\Delta\phi=0.93$ at very small ion densities (see Appendix A) at $\chi=3$. The dielectric constant ε_α in the α phase is twice larger than that ε_β in the β phase. We vary the solvation parameters g_i and the ion densities in the following figures.

In Fig. 2, we show a set of equilibrium profiles for $g_1=-g_2=10$ in the monovalent case.[32] Here, $c_{1\alpha}$ and $c_{1\beta}$ coincide from Eq. (3.1) and is set equal to 2×10^{-4}.[31] The interface thickness ξ is of the order of $5a$, while $\Phi(z)$ changes on the scale of $\kappa_\alpha^{-1}\sim\kappa_\beta^{-1}\sim10a$. Here,

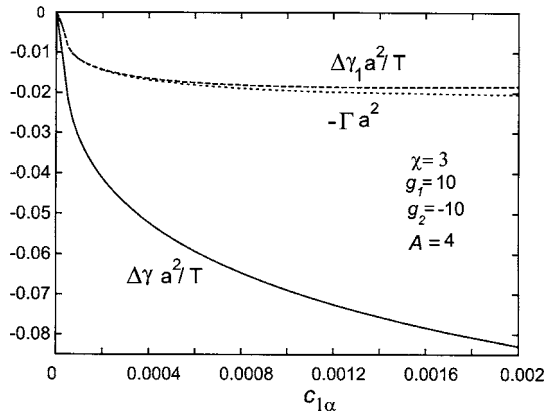

FIG. 3. $a^2\Delta\gamma/T$ and $a^2\Delta\gamma_1/T$ as functions of $c_{1\alpha}$ for strongly hydrophilic and hydrophobic ion pairs, where $\Delta\gamma=\Delta\gamma_1-|\gamma_e|$ and $\Delta\gamma_1=\gamma_1-\gamma_0$. The latter is very close to $-a^2\Gamma$, in agreement with Eq. (2.22). In this case, $|\gamma_e|$ is considerably larger than $|\Delta\gamma_1|$. The parameters are the same as in Fig. 2.

$\Delta\gamma=-0.041Ta^{-2}$ and $\Gamma=0.014a^{-2}$. We can see a marked growth of the electric double layer, which is enhanced with increasing g_1 for the case $g_1=-g_2$. The ion density c_1+c_2 has a deep minimum at the interface position, for which see Fig. 5 also. In our previous work,[13] we obtained milder ion profiles for $g_1=-g_2=4$ and $\chi=2.3$.

In Fig. 3, we examine how the surface tension γ is decreased with increasing $c_{1\alpha}(=c_{1\beta})$, where $g_1=-g_2=10$, as in Fig. 2. We notice the following. (i) The changes $\Delta\gamma=\gamma-\gamma_0$ and $\Delta\gamma_1=\gamma_1-\gamma_0$ are both proportional to $c_{1\alpha}^{1/2}$ at small $c_{1\alpha}$. Here, $|\Delta\gamma|/c_{1\alpha}^{1/2}$ is of the order of unity, so $\Delta\gamma$ is appreciable even for a very small $c_{1\alpha}$. On the other hand, for hydrophilic ion pairs,[13] $\Delta\gamma\cong A_\lambda c_{1\alpha}T/a^2>0$ with the coefficient A_λ being of the order of unity, which is consistent with the well-known surface tension increase for water-air interfaces with salt. (ii) Comparing $\Delta\gamma_1$ and $\Delta\gamma=\Delta\gamma_1+\gamma_e$, we recognize that γ_e is a dominant negative contribution in this case. (iii) We confirm that Eq. (2.22) holds excellently (see Appendix A).

In Fig. 4, we display $\Delta\gamma$ and Γ as functions of g_2 in the range $[-10, 10]$ at $g_1=10$. For $g_2>0$, we have the usual behavior $\Delta\gamma>0$ and $\Gamma<0$. For $g_2<0$, their signs are reversed and their magnitudes are increased dramatically.

B. Analysis using the Poisson–Boltzmann equation

Since γ_e is dominant in Fig. 3, we seek its approximate expression to examine its overall behavior. To this end, we

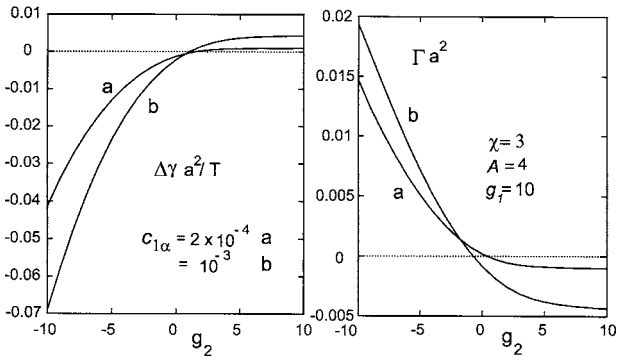

FIG. 4. $a^2\Delta\gamma/T$ (left) and $a^2\Gamma$ (right) vs g_2 for (a)$c_{1\alpha}=2\times10^{-4}$ and (b)10^{-3}, where $\chi=3$, $A=4$, and $g_1=10$. Anions are hydrophilic for $g_2>0$ and hydrophobic for $g_2<0$. The Gibbs relation $\Delta\gamma\cong-T\Gamma$ holds for hydrophilic pairs but does not hold for $-g_2\gg1$ due to increasing $|\gamma_e|$.

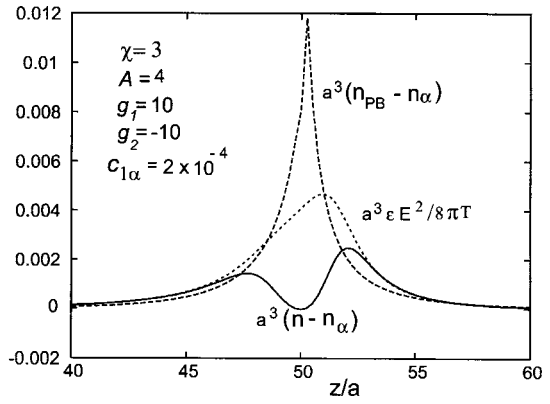

FIG. 5. The normalized electrostatic energy density $a^3\varepsilon(\phi)E(z)^2/8\pi T$ and ion density deviation $a^3(n(z)-n_\alpha)$ calculated numerically, which are compared to the Poisson–Boltzmann solution $a^3(n_{PB}(z)-n_\alpha)$ in Eq. (3.4). The z integration and division by $-a^3/T$ of the first quantity is equal to γ_e in Eq. (2.20) and that of the third quantity is equal to γ_e^{PB} in Eq. (3.7). Here, $\chi=3$, $A=4$, and $c_{1\alpha}=c_{1\beta}=2\times10^{-4}$.

consider situations in which the image interaction is not crucial, the ion densities are very low, and the ions are monovalent. Then, far from the interface position $|z-z_{int}|>\xi$, the ion distributions obey the nonlinear Poisson–Boltzmann equation. That is, for the normalized potential $U(z)=e\Phi(z)/T$, we assume $dU(z)^2/dz^2=\kappa_\beta^2\sinh(U(z)-U_\beta)$ in the region $z>z_{int}$ and $dU(z)^2/dz^2=\kappa_\alpha^2\sinh(U(z)-U_\alpha)$ in the region $z<z_{int}$, where $U_K=e\Phi_K/T$ and $\kappa_K=(4\pi n_K e^2/\varepsilon_K T)^{1/2}$ (=Debye wave number) in the two phases, $K=\alpha$ and β. Here, we supposed the thin interface limit $\xi\to0$.

The resultant electric potential Φ_{PB} is then given by

$$\Phi_{PB}(z)=\Phi_K+\frac{2T}{e}\ln\left[\frac{1+d_K e^{-\kappa_K|z-z_{int}|}}{1-d_K e^{-\kappa_K|z-z_{int}|}}\right], \tag{3.3}$$

where $K=\alpha$ in the region $z<z_{int}$ and $K=\beta$ in the region $z>z_{int}$. The coefficients d_α and d_β are determined from the continuity of Φ_{PB} and $\varepsilon d\Phi_{PB}/dz$ at $z=z_{int}$. In this approximation, the electrostatic energy density divided by T and the ion number density coincide as

$$\frac{\varepsilon E_{PB}^2}{8\pi T}=n_{PB}(z)-n_K=\frac{8n_K d_K^2 e^{-2\kappa_K|z-z_{int}|}}{[1-d_K^2 e^{-2\kappa_K|z-z_{int}|}]^2}, \tag{3.4}$$

where $E_{PB}=-d\Phi_{PB}/dz$ is the electric field and $n_{PB}(z)=n_K\cosh[U(z)-U_K]$ is the number density with $n_K=n_{1K}+n_{2K}$ being the bulk densities. The potential value at the interface position is given by

$$\frac{e}{T}[\Phi_\alpha-\Phi(z_{int})]=\ln\left[\frac{1+be^{e\Delta\Phi/2T}}{1+be^{-e\Delta\Phi/2T}}\right], \tag{3.5}$$

where $b=\varepsilon_\beta\kappa_\beta/\varepsilon_\alpha\kappa_\alpha=n_\beta\kappa_\alpha/n_\alpha\kappa_\beta$ with ε_α and ε_β being the dielectric constants in the bulk phases. In our scheme, Eqs. (3.1) and (3.2) give $e\Delta\Phi/2T=(g_1-g_2)\Delta\phi/4$ and

$$b=(\varepsilon_\beta/\varepsilon_\alpha)^{1/2}\exp[-(g_1+g_2)\Delta\phi/4]. \tag{3.6}$$

Note that $\Delta\Phi$ and b are independent of the ion density.

In Fig. 5, we compare numerically calculated $n-n_\alpha$ and $\varepsilon E^2/8\pi$ with the Poisson–Boltzmann solution $\varepsilon E_{PB}^2/8\pi T=n_{PB}-n_\alpha$ in Eq. (3.4). Here, $\chi=3$, $A=4$, and $c_{1\alpha}=c_{1\beta}=2\times10^{-4}$, for which the image interaction is not

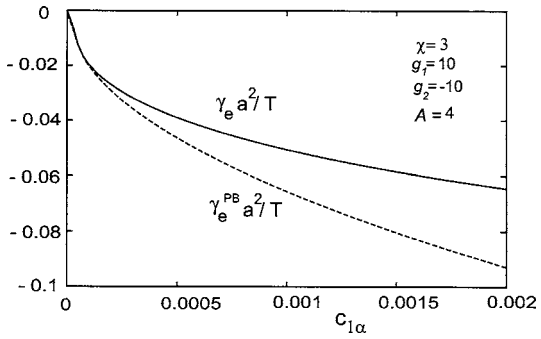

FIG. 6. Numerical $a^2\gamma_e/T$ in Eq. (2.20) and approximate $a^2\gamma_e^{\rm PB}/T$ in Eq. (3.7) as functions of $c_{1\alpha}$, which agree at small $c_{1\alpha}(\lesssim 10^{-4})$.

severe, as shown in Fig. 1. Far from the interface, the Poisson–Boltzmann solution is a good approximation for these two quantities, while at $z\sim z_{\rm int}$, it neglects the double-layer structure and cannot describe the deep minimum of $n-n_\alpha$. We notice that the z integration of $\varepsilon E_{\rm PB}^2/8\pi T=n_{\rm PB}-n_\alpha$ is close to that of $\varepsilon E^2/8\pi$ but is a few times larger than that of Γ in this case. Hence, we approximate γ_e in Eq. (2.20) as the integral of $-\varepsilon E_{\rm PB}^2/8\pi T=-n_{\rm PB}+n_\alpha$, as denoted by $\gamma_e^{\rm PB}$. Some calculations yield

$$\frac{\gamma_e^{\rm PB}}{T}=\frac{2n_\alpha}{\kappa_\alpha}\left[1+b-\sqrt{1+b^2+2b\cosh\left(\frac{e\Delta\Phi}{2T}\right)}\right]$$
$$=-A_s(n_\alpha/\ell_{B\alpha})^{1/2}, \tag{3.7}$$

where b is defined by Eq. (3.6) and $\ell_{B\alpha}=e^2/\varepsilon_\alpha T$ is the Bjerrum length in the α phase. In the second line, the dimensionless coefficient A_s is determined by b and $e\Delta\Phi/T$ and is independent of the ion density n_α, so $\gamma_e^{\rm PB}\propto -n_\alpha^{1/2}$. Thus, we obtain the result $\Delta\gamma\propto -n_\alpha^{1/2}$ at low ion densities for asymmetric ion pairs $g_1\neq g_2$. For small $e\Delta\Phi/T$, we have $\gamma_e\sim -(\Delta\Phi)^2\varepsilon_\alpha\kappa_\alpha/4\pi$ in accord with the argument at the end of Sec. II. Also, the excess adsorption Γ should exhibit this ion density dependence, since the long-range tail of $n-n_\alpha$ and that of $n_{PB}-n_\alpha$ should coincide.

In the case $g_1\geq -g_2\gg 1$, we have $e\Delta\Phi/T=(g_1+|g_2|)\Delta\phi/2$ and $b\ll e^{e\Delta\Phi/2T}$ in Eq. (3.7). Then,

$$A_s\cong \pi^{-1/2}(\varepsilon_\beta/\varepsilon_\alpha)^{1/4}e^{|g_2|\Delta\phi/4}, \tag{3.8}$$

which grows with increasing g_1 and $|g_2|$. In Fig. 3, we notice that the coefficient in front of $c_{1\alpha}^{1/2}$ in $\Delta\gamma a^2/T$ can be of the order of unity, which is equal to $A_s(\pi/4A)^{1/2}$ from Eq. (3.7). In Fig. 6, we compare this approximate $\Delta\gamma_e^{\rm PB}$ and the numerical $\Delta\gamma_e$ for $g_1=-g_2=10$ as functions of $c_{1\alpha}$. Agreement is excellent for $c_{1\alpha}\lesssim 10^{-4}$, while $|\Delta\gamma_e^{\rm PB}|$ is larger than $|\Delta\gamma_e|$ for larger $c_{1\alpha}$.

C. Hydrophilic ion pairs

On the basis of the Poisson–Boltzmann theory, we may also examine the usual case of hydrophilic ion pairs, where g_1 and g_2 are both considerably larger than unity with $g_1>g_2$. (Here, $\Delta\gamma_e^{\rm PB}=0$ for $g_1=g_2$.) Then, we have $n_\alpha\gg n_\beta$ and $b\ll 1$ not close to the critical point, leading to

$$\Delta\gamma_e^{\rm PB}\cong -2T[\cosh(e\Delta\Phi/2T)-1]bn_\alpha/\kappa_\alpha, \tag{3.9}$$

where $bn_\alpha/\kappa_\alpha=n_\beta/\kappa_\beta\propto n_\beta^{1/2}$. Here, the right-hand side is the integration result in the β region since that in the α region is smaller by b. From Eq. (3.5), $\Phi_\alpha-\Phi(z)\propto b$ in the α region. If $(g_1-g_2)\Delta\phi>1$, we find $|\Delta\gamma_e^{\rm PB}|a^2/T\sim e^{-g_2\Delta\phi/2}(c_{1\alpha}/A)^{1/2}$, where A is defined by Eq. (2.6). Thus, together with a positive $\Delta\gamma_1$, we obtain the following expression:

$$\Delta\gamma\cong -A_sT(n_\alpha/\ell_{B\alpha})^{1/2}+\lambda_sTn_\alpha. \tag{3.10}$$

Here, the coefficient A_s is small $(\sim(\varepsilon_\beta/\varepsilon_\alpha)^{1/2}e^{-g_2\Delta\phi/2})$. The second term is of the well-known form that accounts for the ion depletion near the interface. With this expression, $\Delta\gamma$ should exhibit a small minimum given by

$$(\Delta\gamma)_{\rm min}=-T\lambda_sn_m \tag{3.11}$$

at $n=n_m=(A_s/2\lambda_s)^2/\ell_{B\alpha}$. As an example, let the ion concentration giving this minimum be 1 mM in the water-rich phase.[31] Then, we obtain $A_s=1.2\times 10^{-2}$ by setting $\lambda_s=3$ Å and $\ell_{B\alpha}=7$ Å.

For water-air interfaces, Jones and Ray[5] found a negative minimum in $\Delta\gamma$ of the order of $-10^{-4}\gamma_0$. Their data can well be fitted into Eq. (3.10) with $A_s\sim 10^{-2}$. However, we have assumed appreciable ion densities even in the less polar β region. That is, our 1D calculations are justified only when the screening length κ_β^{-1} in the β region is much shorter than any characteristic lengths in experiments, which are the inverse curvature of the meniscus or the wavelength of capillary waves, for example. In literature,[1–3,9,10] ions are treated to be nonexistent in the air region, so in our scheme we do not still understand the Jones–Ray effect.

Here, it is worth noting that Nicols and Pratt[33] theoretically derived the square-root dependence of $\Delta\gamma$ as the low-density asymptotic law when ions are appreciably soluble both in the two phases. They calculated the ion density deviations decaying on the scale of the screening length far from the interface, which vanish as $\kappa_\beta\to 0$, as in our theory.

IV. THREE SPECIES OF IONS

Next, we consider the ion distributions in the case of three ion species for water-oil interfaces. As in the experiment,[15] we assume monovalent ions with charges $Q_1=e, Q_2=-e$, and $Q_3=-e$ for the three species. Namely, the first species consists of monovalent cations, while the second and third species are monovalent anions. The ion distributions are very complicated and numerical calculations are needed for their analysis.

Before presenting numerical results, we first examine the potential difference $\Delta\Phi$, which is determined from Eqs. (2.12) and (2.13).[11,28] For example, in terms of the ion densities in the α phase, it follows the equation for $\Delta\Phi$ in the form

$$c_{1\alpha}e^{2e\Delta\Phi/T}=c_{2\alpha}e^{(g_1-g_2)\Delta\phi}+c_{3\alpha}e^{(g_1-g_3)\Delta\phi}, \tag{4.1}$$

where $c_{1\alpha}=c_{2\alpha}+c_{3\alpha}$. This yields Eq. (3.2) for $c_{3\alpha}=0$ in the monovalent case.

However, in the experiment,[15] the third species (TPB^-) was strongly hydrophobic such that $c_{3\alpha}\ll c_{3\beta}$ was realized,

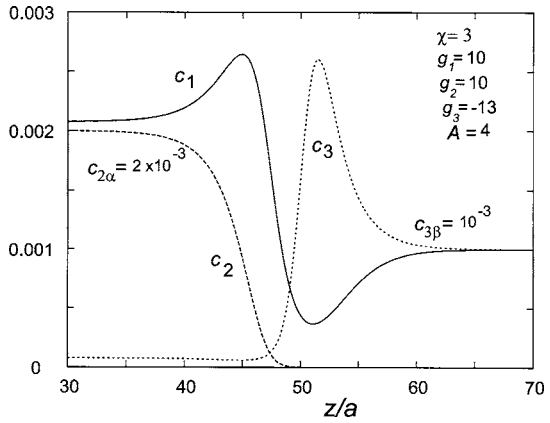

FIG. 7. The normalized ion densities $c_1(z)$, $c_2(z)$, and $c_3(z)$ of three ion species in the monovalent case for $c_{2\alpha}=2\times10^{-3}$ and $c_{3\beta}=10^{-3}$. The species 1 and 2 are hydrophilic as $g_1=g_2=10$, while the third species is hydrophobic as $g_3=-13$. Then, $c_{2\beta}\cong0$ and $c_{3\alpha}\ll1$.

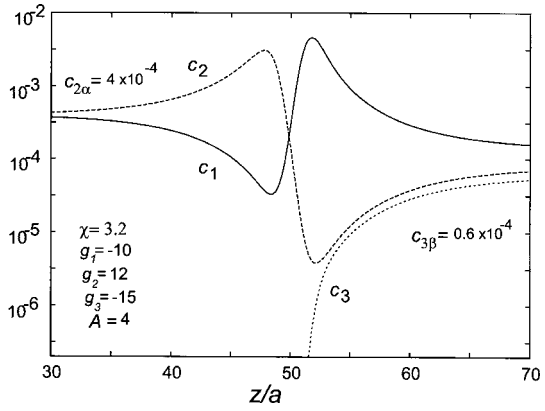

FIG. 8. The normalized ion densities $c_1(z)$, $c_2(z)$, and $c_3(z)$ in the presence of three ion species with $g_1=-10$, $g_2=12$, and $g_3=-13$, respectively, on a semilogarithmic scale, resembling to those in the experiment (Ref. 15). The third species does not penetrate into the α region.

while the second species (Br^-) was hydrophilic. Supposing such cases, let us assume $g_2>0$ and $g_3<0$ and choose $c_{2\alpha}$ and $c_{3\beta}$ as control parameters. If we set

$$X=\exp[e\Delta\Phi/T-(g_1-g_2)\Delta\phi/2], \tag{4.2}$$

Eq. (4.1) becomes a cubic equation,

$$X-X^{-1}=2R[1-X^2e^{(g_3-g_2)\Delta\phi}], \tag{4.3}$$

where $R(\propto c_{3\beta})$ is defined by

$$R=e^{(g_1+g_2)\Delta\phi/2}c_{3\beta}/2c_{2\alpha}. \tag{4.4}$$

The right-hand side of Eq. (4.3) arises in the presence of the third species. We may well assume $X^2e^{(g_3-g_2)\Delta\phi}\ll1$ for large $|g_3|\gg1$ to obtain $X\cong R+\sqrt{1+R^2}$ or

$$\frac{e}{T}\Delta\Phi\cong\frac{1}{2}(g_1-g_2)\Delta\phi+\ln(R+\sqrt{1+R^2}). \tag{4.5}$$

If $(g_1+g_2)\Delta\phi\gg1$, we readily reach the new regime $R\gg1$ even for small $c_{3\beta}$, where $X\cong2R$ holds and $X^2e^{(g_3-g_2)\Delta\phi}\cong(c_{3\beta}/c_{2\alpha})^2e^{(g_1+g_3)\Delta\phi}$ needs to be small. That is, we find

$$\frac{e}{T}\Delta\Phi\cong g_1\Delta\phi+\ln(c_{3\beta}/c_{2\alpha}) \tag{4.6}$$

for $e^{-(g_1+g_2)\Delta\phi/2}\ll c_{3\beta}/c_{2\alpha}\ll e^{-(g_1+g_3)\Delta\phi/2}$. In this case, $c_{1\alpha}\cong c_{2\alpha}$, $c_{1\beta}\cong c_{3\beta}$, $c_{2\beta}\cong e^{-(g_1+g_2)\Delta\phi}c_{2\alpha}^2/c_{3\beta}\ll c_{3\beta}$, and $c_{3\alpha}\cong e^{(g_1+g_3)\Delta\phi}c_{3\beta}^2/c_{2\alpha}\ll c_{2\alpha}$.

In Fig. 7, we display the ion distributions in the presence of three ion species in the monovalent case with $Q_1=e$, $Q_2=-e$, and $Q_3=-e$. Since the absolute values of g_i are taken to be large, we can see steep and complex variations of the ion distributions around the interface. The first and second species are both hydrophilic but the third one is hydrophobic as $g_1=g_2=10$ and $g_3=-13$. Here, $\chi=3$, $e\Delta\Phi/T=7.92$, and $\gamma=0.446T/a^2$, while $\Delta\Phi=0$ for $c_{3\beta}=0$ since $g_1=g_2$. The peaks of c_1 and c_3 are conspicuous. This is the case discussed in Eq. (4.6) since $X^2e^{(g_3-g_2)\Delta\phi}=1.5\times10^{-2}$ and $R=2.7\times10^3$.

In Fig. 8, the first and third species are hydrophobic but the second species is hydrophilic as $g_1=-10$, $g_2=12$, and $g_3=-15$, where $\chi=3.2$, $e\Delta\Phi/T=7.01$, and $\gamma=0.600T/a^2$ (with $\gamma_0=0.620T/a^2$ at $\chi=3.2$). Here, c_1 and c_2 exhibit sharp peaks. The ion distributions in this case can be compared with those in the experiment by Luo *et al.*,[15] so the curves are written on a semilogarithmic scale as in their paper. The adopted parameter values are inferred from their experimental data.

V. SUMMARY

The effects of ions in polar fluid mixtures are very complex because of the presence of the electrostatic, solvation, and image interactions. Our continuum theory takes account of these interactions, although it should be inaccurate on the angstrom scale. Our main results are as follows. In Fig. 2, we have illustrated the singular ion distributions around an interface when hydrophilic and hydrophobic ions coexist. We have given the general expression for the surface tension in electrolytes in Eqs. (2.19) and (2.20). In Fig. 3, the resultant surface tension change $\Delta\gamma$ is proportional to the square root of the ion density in the dilute limit. This dependence arises from the fact that the electrostatic field changes over the distance of the screening length far from the interface. When the image interaction is not severe, the electrostatic contribution γ_e to the surface tension can be estimated by the Poisson–Boltzmann result in Eq. (3.7), as demonstrated in Fig. 6. For hydrophilic ion pairs, we propose the expression [Eq. (3.10)] consisting of the negative square-root and positive linear terms. In the presence of three ion species, the ion distributions are very complex as in Figs. 7 and 8, where Fig. 8 corresponds to the experimental result.[15]

Using salts composed of hydrophilic and hydrophobic ions, a large decrease in γ far from the critical point,[11,15] ion distributions near an interface,[15] and a mesophase near the critical point[14] have already been reported. We propose more systematic surface tension measurements of water-oil interfaces with dissimilar cations and anions.

In this paper, we have neglected the clustering of ions. (i) For hydrophilic ions, this effect becomes conspicuous for densities larger than $1M$ in aqueous solutions.[20–22] It is not clear as to how hydrophilic and hydrophobic ions can form clusters with increasing their densities. (ii) It is worth noting that ion aggregation was predicted to occur near the critical

point (even among ions of the same species) because of a long-range interaction mediated by the critical fluctuations (see Appendix A of our previous paper[13]). (iii) For ionic surfactants, the amphiphilic interaction with water and oil needs to be included. Recently, we have found that the adsorption of ionic surfactant and counterions onto a water-oil interface is dramatically enhanced when these two species constitute a hydrophilic and hydrophobic pair producing a large electric double layer.[34]

In the future, we should study the surface tension near the critical point in the presence of hydrophilic and hydrophobic ions with $|g_i| \gg 1$. The mesophase formation realized for such ion pairs near the critical point should also be investigated.[12–14] Dynamics of phase ordering in ionic fluids with the solvation interaction has not yet been explored. Transient relaxations under applied electric field could also be studied.

ACKNOWLEDGMENTS

This work was supported by Grants in Aid for Scientific Research and for the 21st Century COE project (Center for Diversity and Universality in Physics) from the Ministry of Education, Culture, Sports, Science and Technology of Japan.

APPENDIX A: DERIVATION OF THE GIBBS RELATION FOR DILUTE ION DENSITIES

Here, we derive Eq. (2.22) in the Ginzburg–Landau theory for small n. Let $\phi_0(z)$ and h_0 be the composition profile and the chemical potential difference without ions. From Eq. (2.10), the deviation $\delta\phi=\phi-\phi_0$ obeys

$$\left[f_0''(\phi) - C\frac{d^2}{dz^2}\right]\delta\phi = \frac{\varepsilon_1 E^2}{8\pi} + T\sum_i g_i n_i - h_{\rm im} + \delta h \tag{A1}$$

to linear order, where $f_0''=\partial^2 f_0/\partial\phi^2$. For the free energy density in Eq. (2.2), we have $f_0''=[\phi^{-1}(1-\phi)^{-1}-2\chi]T/a^3$. Obviously, the left-hand side of Eq. (A1) vanishes to a linear order if we multiply it by $\phi'=d\phi/dz$ and integrate over z. We can show that the right-hand side also vanishes in the same procedure from $\int dz(\varepsilon_1 E^2\phi'/8\pi+\Phi'\rho)=0$ and $\int dz(h_{\rm im}\phi'+\Sigma_i\mu_{\rm im}Z_i^2 n_i')=0$, where the latter follows from Eq. (4.24) of our previous paper[13] and the primes denote operating d/dz. This orthogonality to ϕ' is the solubility condition of Eq. (A1).[13] From Eqs. (2.13) and (2.18), the deviation $\delta h=h-h_0$ is calculated as

$$\delta h = -T\Delta n/\Delta\phi + \cdots. \tag{A2}$$

The bulk volume fractions are expanded as

$$\phi_K = \phi_{K0} + T\left(\sum_i g_i n_{iK} - \frac{\Delta n}{\Delta\phi}\right)/f_0''(\phi_K) + \cdots, \tag{A3}$$

where $K=\alpha$ and β. ϕ_{K0} are the bulk values without ions. From Eq. (2.19), we may expand γ_1 with respect to $\delta\phi=\phi-\phi_0$ up to second order as

$$\gamma_1 = \gamma_0 - T\Gamma + \int dz\frac{C}{2}(\delta\phi')^2 + \int dz\left[\zeta(z) - \zeta_\alpha - \frac{\Delta\zeta}{\Delta\phi}(\phi(z)-\phi_\alpha)\right] + \cdots, \tag{A4}$$

where $\zeta=f_0''(\phi)(\delta\phi)^2/2$ and $\Delta\zeta=\zeta_\alpha-\zeta_\beta$. The terms that are linear in $\delta\phi$ vanish from the interface equation $h_0=f_0'(\psi_0)-C\phi_0''$ without ions. The third and fourth terms are of the second order in $\delta\phi$ and, if they are neglected, we obtain Eq. (2.22). However, the corrections grow near the critical point.

APPENDIX B: GRAND POTENTIAL AND SURFACE TENSION IN INCOMPRESSIBLE FLUID MIXTURES

In the text, we have neglected the deviation of the number density $n_t=n_A+n_B$ of the solvent from a reference density n_t^0 assuming the common molecular size ($a_A=a_B=a$). More generally, the system is characterized by the solvent densities

$$n_A = n_t\phi, \quad n_B = n_t(1-\phi), \tag{B1}$$

in addition to the ion densities n_1 and n_2. We assume $\phi=n_A/(n_A+n_B)$, so ϕ is also the molar fraction. The density deviation $\delta n_t=n_t-n_t^0$ is small. Hereafter, we suppress the dependence on T.

For nearly incompressible fluid mixtures, the dependence on δn_t may be accounted for if we replace $f_0(\phi)$ in Eq. (2.1) by the Helmholtz free energy density

$$\hat{f}_0(\phi,n_t) = f_0(\phi) + a_0 + a_1(\phi)\delta n_t + \frac{a_2(\phi)}{2}(\delta n_t)^2, \tag{B2}$$

where a_0 is independent of the densities (being dependent only on T), but a_1 and a_2 depend on ϕ (and T). Far from the interface, where the image interaction vanishes and the fluid is homogeneous, the pressure p is given by

$$p = -f_0 - a_0 + a_1 n_t^0 + a_2 n_t^0\delta n_t + T\sum_i n_i \tag{B3}$$

up to first order in δn_t. The last term is the contribution from ions. The coefficient a_2 is inversely proportional to the compressibility $(\partial n_t/\partial p)_{T\phi}/n_t$ and is large such that $a_2\delta n_t$ is appreciable in Eq. (B3), while $a_2(\delta n_t)^2/2$ is small in Eq. (B2). The chemical potentials of the two components $\mu_A=\delta F/\delta n_A$ and $\mu_B=\delta F/\delta n_B$ are expressed as

$$\mu_A = (1-\phi)(h+\Delta h)/n_t + a_1 + a_2\delta n_t,$$
$$\mu_B = -\phi(h+\Delta h)/n_t + a_1 + a_2\delta n_t, \tag{B4}$$

where h is given in Eq. (2.10) and

$$\Delta h = \frac{\partial a_1}{\partial\phi}\delta n_t + \frac{1}{2}\frac{\partial a_2}{\partial\phi}(\delta n_t)^2. \tag{B5}$$

We find $h+\Delta h=n_t(\mu_A-\mu_B)$. The expressions for the ion chemical potentials μ_1 and μ_2 in Eq. (2.8) are unchanged. For nonvanishing δn_t, we define the generalized grand potential density by

$$\hat{\omega} = f + (\hat{f}_0 - f_0) - n_A\mu_A - n_B\mu_B - n_1\mu_1 - n_2\mu_2$$
$$= \omega - n_t\mu_B - \phi\Delta h + (\hat{f}_0 - f_0), \tag{B6}$$

where ω is the grand potential density in Eq. (2.17) in the incompressible case and use has been made of $n_A\mu_A + n_B\mu_B = n_t\mu_B + \phi(h+\Delta h)$. In the bulk regions, $\hat{\omega}$ should be equal to the minus of the pressure p. We assume that the electric field vanishes far from the interface and there is no contribution of the Maxwell stress tensor.

In particular, when the fluid is separated by a planar interface, the four chemical potentials, μ_A, μ_B, μ_1, and μ_2, become homogeneous. Here, $\hat{\omega}$ tends to a constant $-p_\infty$ as $z \to \pm\infty$. In the right-hand side of Eq. (B6), we may replace n_t by n_t^0 and $\hat{f}_0 - f_0$ by a_0 for small δn_t. Then, as assumed in the text, ω tends to $\omega_\infty = -p_\infty + n_t^0\mu_B - a_0$ as $z \to \pm\infty$ and the surface tension is expressed as

$$\gamma = \int dz[\hat{\omega}(z) + p_\infty] \cong \int dz[\omega(z) - \omega_\infty], \tag{B7}$$

where the first line is general and the second line is its incompressible limit $\delta n_t \to 0$.

We also consider an equilibrium spherical droplet with radius R in one of the two phases, say, the α phase. In this case, the total Helmholtz free energy F is minimized for the given system volume V and the total particle numbers, N_A, N_B, and $N_1 = N_2$. The densities inside and outside the droplet are then determined such that the four chemical potentials become homogeneous (see Chapter 9.1 of the book by the present author[23]). We furthermore minimize F with respect to R in the presence of the surface free energy $4\pi\gamma R^2$. This yields the famous pressure difference $\Delta p = p_\alpha - p_\beta = 2\gamma/R$ (the Laplace law). Thus, there arises a difference in the bulk values of ω given by

$$-\omega_\alpha + \omega_\beta = \Delta p = 2\gamma/R, \tag{B8}$$

which holds in the limit $\delta n_t \to 0$. As $R \to \infty$, we have $\omega_\alpha = \omega_\beta = \omega_\infty$.

[1] C. Wagner, Phys. Z. **25**, 474 (1924).
[2] L. Onsager and N. N. T. Samaras, J. Chem. Phys. **2**, 528 (1934).
[3] Y. Levin and J. E. Flores-Mena, Europhys. Lett. **56**, 187 (2001).
[4] J. N. Israelachvili, *Intermolecular and Surface Forces* (Academic, London, 1991).
[5] G. Jones and W. A. Ray, J. Am. Chem. Soc. **59**, 187 (1937); G. Jones and W. A. Ray, *ibid.* **63**, 288 (1941); G. Jones and W. A. Ray, *ibid.* **63**, 3262 (1941).
[6] N. Matubayasi, H. Matsuo, K. Yamamoto, S. Yamaguchi, and A. Matuzawa, J. Colloid Interface Sci. **209**, 398 (1999).
[7] H. Ohshima and H. Matsubara, Colloid Polym. Sci. **282**, 1044 (2002).
[8] P. B. Petersen and R. J. Saykally, J. Am. Chem. Soc. **127**, 15446 (2005).
[9] K. A. Karraker and C. J. Radke, Adv. Colloid Interface Sci. **96**, 231 (2002).
[10] M. Manciu and E. Ruckenstein, Adv. Colloid Interface Sci. **105**, 63 (2003).
[11] J. D. Reid, O. R. Melroy, and R. P. Buck, J. Electroanal. Chem. Interfacial Electrochem. **147**, 71 (1983).
[12] A. Onuki and H. Kitamura, J. Chem. Phys. **121**, 3143 (2004).
[13] A. Onuki, Phys. Rev. E **73**, 021506 (2006).
[14] K. Sadakane, H. Seto, H. Endo, and M. Shibayama, J. Phys. Soc. Jpn. **76**, 113602 (2007).
[15] G. Luo, S. Malkova, J. Yoon, D. G. Schultz, B. Lin, M. Meron, I. Benjamin, P. Vanysek, and M. L. Schlossman, Science **311**, 216 (2006).
[16] I. Benjamin, Chem. Rev. (Washington, D.C.) **106**, 1212 (2006).
[17] P. Jungwirth and D. J. Tobias, Chem. Rev. (Washington, D.C.) **106**, 1259 (2006).
[18] J. W. Gibbs, *Collected Works* (Yale University Press, New Haven, CT, 1957), Vol. 1, pp. 219–331.
[19] J. S. Rowlinson and B. Widom, *Molecular Theory of Capillarity* (Clarendon, Oxford, 1989).
[20] L. Degrève and F. M. Mazzé, Mol. Phys. **101**, 1443 (2003).
[21] A. A. Chen and R. V. Pappu, J. Phys. Chem. B **111**, 6469 (2007).
[22] S. A. Hassan, Phys. Rev. E **77**, 031501 (2008).
[23] A. Onuki, *Phase Transition Dynamics* (Cambridge University Press, Cambridge, 2002).
[24] S. A. Safran, *Statistical Thermodynamics of Surfaces, Interfaces, and Membranes* (Addison Wesley, Reading, MA, 1994).
[25] P. Debye and K. Kleboth, J. Chem. Phys. **42**, 3155 (1965).
[26] M. Gros, S. Gromb, and C. Gavach, J. Electroanal. Chem. Interfacial Electrochem. **89**, 29 (1978).
[27] J. Koryta, Electrochim. Acta **24**, 293 (1979); **29**, 445 (1984).
[28] L. Q. Hung, J. Electroanal. Chem. Interfacial Electrochem. **115**, 159 (1980); **149**, 1 (1983).
[29] T. Osakai and K. Ebina, J. Phys. Chem. B **102**, 5691 (1998).
[30] The Gibbs transfer energy $\Delta G^i_{\alpha\beta}$ per mole is 34.2 for Na^+, 67.3 for Ca^{2+}, and −35.9 for BPh_4^- in units of kJ for strongly segregated water-nitrobenzene at room temperatures (Ref. 28). Dividing them by the Avogadro number gives $\Delta\mu^i_{\alpha\beta}$ per particle.
[31] The density of 1 mM salt is $n = 6\times10^{17}$ cm^{-3}. If $a = 3$ Å, the normalized density $c = a^3 n$ is equal to 1.6×10^{-5}.
[32] A mesoscopic phase is realized if a parameter γ_p representing the asymmetry of the ion solvation exceeds unity (Refs. 12 and 13). For $C = T\chi/a^2$, it is equal to $|g_1 - g_2|/8\sqrt{\chi A}$ in the monovalent case. In particular, we have $\gamma_p = 5/4\sqrt{3} < 1$ for the parameter values in Fig. 2, $g_1 = -g_2 = 10$, $\chi = 3$, and $A = 4$.
[33] A. L. Nicols and L. R. Pratt, J. Chem. Phys. **80**, 6225 (1984).
[34] A. Onuki, Europhys. Lett. **82**, 58002 (2008).